Title
Compartmentalized Toxoplasma EB1 bundles spindle microtubules to secure accurate chromosome segregation

Journal
Molecular Biology of the Cell, 26(25)

ISSN
1059-1524

Authors
Chen, Chun-Ti
Kelly, Megan
de Leon, Jessica
et al.

Publication Date
2015-12-15

DOI
10.1091/mbc.e15-06-0437

Peer reviewed

Compartmentalized *Toxoplasma* EB1 bundles spindle microtubules to secure accurate chromosome segregation

Chun-Ti Chen[a], Megan Kelly[a,*], Jessica de Leon[b,†], Belinda Nwagbara[a], Patrick Ebbert[a], David J. P. Ferguson[c], Laura Anne Lowery[a], Naomi Morrissette[b], and Marc-Jan Gubbels[a]

[a]Department of Biology, Boston College, Chestnut Hill, MA 02467; [b]Molecular Biology and Biochemistry, University of California, Irvine, Irvine, CA 92697; [c]Nuffield Department of Clinical Laboratory Science, University of Oxford, John Radcliffe Hospital, Oxford OX3 9DU, United Kingdom

ABSTRACT ***Toxoplasma gondii*** **replicates asexually by a unique internal budding process characterized by interwoven closed mitosis and cytokinesis. Although it is known that the centrosome coordinates these processes, the spatiotemporal organization of mitosis remains poorly defined. Here we demonstrate that centrosome positioning around the nucleus may signal spindle assembly: spindle microtubules (MTs) are first assembled when the centrosome moves to the basal side and become extensively acetylated after the duplicated centrosomes reposition to the apical side. We also tracked the spindle MTs using the MT plus end–binding protein TgEB1. Endowed by a C-terminal NLS, TgEB1 resides in the nucleoplasm in interphase and associates with the spindle MTs during mitosis. TgEB1 also associates with the subpellicular MTs at the growing end of daughter buds toward the completion of karyokinesis. Depletion of TgEB1 results in escalated disintegration of kinetochore clustering. Furthermore, we show that TgEB1's MT association in *Toxoplasma* and in a heterologous system (*Xenopus*) is based on the same principles. Finally, overexpression of a high-MT-affinity TgEB1 mutant promotes the formation of overstabilized MT bundles, resulting in avulsion of otherwise tightly clustered kinetochores. Overall we conclude that centrosome position controls spindle activity and that TgEB1 is critical for mitotic integrity.**

Monitoring Editor
Kerry S. Bloom
University of North Carolina

Received: Jun 25, 2015
Revised: Oct 2, 2015
Accepted: Oct 2, 2015

INTRODUCTION

Toxoplasma gondii is a unicellular eukaryotic pathogen infecting all warm-blooded animals. The invasive tachyzoite form of this obligate intracellular parasite is capable of infecting a boundless variety of nucleated cell types. The parasite replicates within a membrane-bound vacuole sequestering it from the host cell. When all resources are consumed, the parasites egress, lysing the host cell in the process. The released parasite progeny invade new host cells and continue the cycle, which leads to extensive tissue damage and clinical disease if uncontrolled by a potent immune response (Montoya and Liesenfeld, 2004). Vegetative (asexual) replication of the tachyzoite stage unfolds by closed mitosis coupled with internal budding to produce two daughter cells per division round (Francia and Striepen, 2014). The *Toxoplasma* centrosome serves as a central hub, functioning as a microtubule-organizing center (MTOC) at the spindle poles while in addition providing the platform for the assembly of daughter cell cytoskeletal components (Chen and Gubbels, 2013). A striated fiber assemblin structure anchors the centrosome in the growing daughter cytoskeleton (Francia *et al.*, 2012). Besides the mitotic spindle, microtubules (MTs) are also present in the apical conoid complex, in two central microtubules anchored apically, and in a set of 22 subpellicular MTs emanating from the apical polar ring, which extends along approximately two-thirds of the parasite length. Assembly of daughter cytoskeletal components proceeds in an apical-to-basal direction concurrent with mitosis and the partitioning of

This article was published online ahead of print in MBoC in Press (http://www.molbiolcell.org/cgi/doi/10.1091/mbc.E15-06-0437) on October 14, 2015.

Present addresses: *Sanofi-Genzyme, Framingham, MA 01701; †Department of Public Health, San Bernardino County, San Bernardino, CA 92415.

Address correspondence to: Naomi Morrissette (nmorriss@uci.edu), Marc-Jan Gubbels (gubbelsj@bc.edu).

Abbreviations used: ATc, anhydrotetracycline; EB1, end–binding protein 1; MORN1, membrane occupation and recognition nexus protein 1; MT, microtubule; NLS, nuclear localization signal.

the nucleus, Golgi apparatus, plastid, and finally mitochondria into the elongating daughter cells (Nishi *et al.*, 2008). Whereas many components and processes of the daughter bud cytoskeleton have been identified and characterized in recent years (Anderson-White *et al.*, 2012; Tran *et al.*, 2012), the regulation of mitosis and the mitotic spindle has been understudied.

At the ultrastructural level, many features distinguish mitosis in *Toxoplasma* from mitosis in vertebrate host cells. *Toxoplasma* undergoes a closed mitosis by which the spindle poles are positioned eccentrically on the apical end of the nucleus. Spindle MTs originate in close apposition to the centrosome residing in the cytoplasm and penetrate the nuclear envelope through a specialized nuclear membrane compartment known as the centrocone (Gubbels *et al.*, 2006). Furthermore, the 14 chromosomes are kept clustered and associated with the centrocone, which is maintained throughout the cell and mitotic cycles (Gubbels *et al.*, 2006; Brooks *et al.*, 2011). The Ndc80 complex at the MT–kinetochore interface is conserved in *T. gondii*. Strikingly, the Ndc80 complex is maintained throughout the cell cycle although it is critical only during mitosis, when it is essential to anchor the nucleus to the centrosome (Farrell and Gubbels, 2014). Given this peculiarity, we set out to define the dynamics of the spindle MTs throughout the cell cycle, in particular during mitosis.

MT end–binding proteins (EBs) are evolutionarily conserved proteins found in all eukaryotic cells that bind to the growing end of MTs (Beinhauer *et al.*, 1997; Lee *et al.*, 2000; Bu and Su, 2001; Komaki *et al.*, 2010). The N-terminal calponin homology (CH) domain is the most conserved region and directly associates with the growing MT plus end. The C-terminal coiled-coil domain mediates parallel dimerization and partially overlaps with an EB1-homology motif, which interacts with plus end–tracking proteins to regulate MT dynamics (Akhmanova and Steinmetz, 2008; Komarova *et al.*, 2009). The association of EB1 with MTs promotes their stability and extension. Besides MT-associated proteins, spindle MT stability is further controlled by posttranslational modifications (Piperno *et al.*, 1987; Verhey and Gaertig, 2007; Janke and Kneussel, 2010). In particular, acetylation of the conserved Lys-40 residue in α-tubulin is associated with enhanced stability.

In this study, we find that tubulin is first recruited to the centrocone in late G1 just before centrosome duplication at the basal side of the nucleus, highlighting an unusual and previously unidentified spatial regulatory mechanism. TgEB1 resides in the nucleoplasm during interphase, transitions to the spindle MTs upon spindle assembly, and, after completion of karyokinesis, is briefly associated with the ends of the subpellicular MTs. Nuclear localization is unique to TgEB1 and is directed by its unique C-terminal extension. Manipulation of TgEB1's affinity for MT binding by point mutations shows that the spindle MTs are highly dynamic structures that are tightly regulated. We further find that acetylation on α-tubulin is associated with spindle stability. Finally, by ablation of TgEB1, we demonstrate its role in clustering the kinetochores, with a minor role in cytokinesis. In conclusion, our data demonstrate that *Toxoplasma* spindle assembly is tightly coordinated with the centrosome cycle and that both tubulin acetylation and nuclear-sequestered TgEB1 control the stability of MTs to secure faithful mitosis.

RESULTS

Centrosome repositioning precedes spindle assembly

The paradoxical observation that the persistent clustering of all 14 kinetochores at the centrocone during interphase was independent of the Ndc80 complex and thus of the MTs led us to assess the presence of spindle MTs throughout the *Toxoplasma* cell cycle (Gubbels *et al.*, 2006; Brooks *et al.*, 2011; Farrell and Gubbels, 2014). We set out by using tubulin antibodies and established cell-cycle markers to investigate spindle MTs in the centrocone. Because the centrosome duplicates late in the G1/S phase transition of the cell cycle after its migration to the basal end of the nucleus (Hartmann *et al.*, 2006), we labeled the centrosome in combination with tubulin antisera to determine the timing of spindle assembly. As shown in Figure 1, A and B, during early G1 phase (single centrosome at the apical end of the nucleus), no β-tubulin signal was observed in the nucleus. β-Tubulin first appeared at the spindle pole just before duplication of the centrosome at the basal end of the nucleus (Figure 1A, late G1 and G1/S phases). We confirmed recruitment of β-tubulin to the centrocone by using the membrane occupation and recognition nexus protein MORN1 as a marker, which highlights the centrocone throughout the cell cycle (Gubbels *et al.*, 2006). β-Tubulin indeed colocalizes with MORN1 when it first appears and actually remains continuously associated with it throughout mitosis and karyokinesis. The schematic in Figure 1C summarizes the four cell-cycle stages in early G1 though S phases shown in Figure 1A.

Although the centrocone was believed to be invariably located at the apical end of the nucleus, the centrosome has been reported to migrate to the basal end of the nucleus before duplication (Hartmann *et al.*, 2006). To consolidate our new observation of a comigrating centrocone, we established how the spindle MTs are coordinated with progression through mitosis and cell division. The kinetochore marker Nuf2 (Farrell and Gubbels, 2014) comigrates with β-tubulin to the basal end of the nucleus (Figure 1D). Subsequently, we localized the apicoplast, a nonphotosynthetic plastid dividing in association with the centrosome (Striepen *et al.*, 2000). Of note, the plastid remains apical of the nucleus when the spindle is located at the basal side of nucleus (Figure 1E). This observation is consistent with a report on the temporal dissociation of the apicoplast from the centrosome (Vaishnava *et al.*, 2005). On the basis of these results, we conclude that the centrocone with associated kinetochores comigrates with the centrosome to the basal side of the nucleus, which may provide a spatial cue for the assembly of spindle MTs.

Dynamics of α-tubulin acetylation during mitosis

Acetylation of lysine 40 (K40) is an evolutionarily conserved posttranslational modification of α-tubulin associated with increased stability of various MT populations, including the mitotic spindle (Piperno *et al.*, 1987; Verhey and Gaertig, 2007; Janke and Bulinski, 2011). Because K40 acetylation has been detected in *Toxoplasma* (Xiao *et al.*, 2010), we assessed whether it could be involved in regulating spindle dynamics in *T. gondii* tachyzoites. To test this, we costained for β-tubulin– and acetylated (Ac)-α-tubulin–specific antibodies. Localization of Ac-α-tubulin was nearly identical to that of β-tubulin at the subpellicular MTs, the centrocone, and the subpellicular MTs in the newly formed daughter buds (Figure 2A). However, in the centrocone, no or very limited Ac-α-tubulin signal could be detected when β-tubulin was present at the basal end of the nucleus (Figure 2A, second from top). Ac-α-tubulin in the spindle pole increases dramatically upon reorientation to the apical end (Figure 2A, S phase) and continues throughout mitosis when β-tubulin is visible as a bar (Figure 2A, mitosis), likely representing both the kinetochore and interpolar spindle MTs. Finally, the Ac-α-tubulin signal wanes before the β-tubulin signal upon completion of karyokinesis, during daughter bud elongation (Figure 2A, bottom). To better understand the appearance and the timing of spindle acetylation, we quantified the position and localization of acetylated

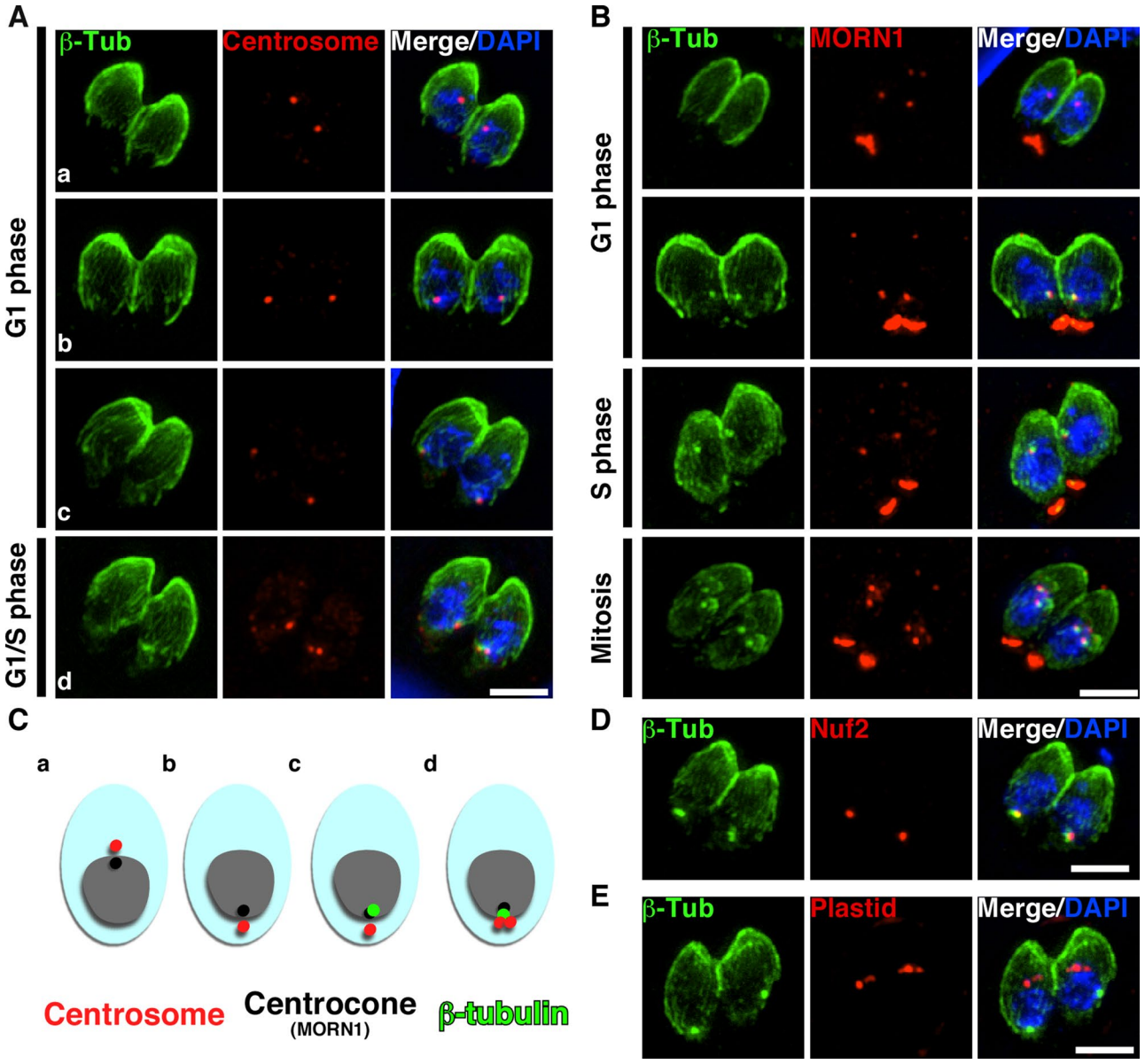

FIGURE 1: Spindle MT assembly in space and time. (A) Spindle assembly initiates when the centrosome rotates to the basal side of the nucleus. Wild-type parasites expressing DDmyc-Centrin1 stabilized with Shield1 were costained with cMyc (marking the centrosome in red) and β-tubulin antisera. The cell division cycle progresses from top to bottom, and phases are as indicated on the left. (B) The centrocone rotates along with the spindle MT upon assembly at the basal end of nucleus. Parasites stably expressing myc2-MORN1 were costained with cMyc and β-tubulin antisera. The cell division cycle progresses from top to bottom, and phases are as indicated on the left. (C) Schematic representation of the results in A and B. The centrosome is marked in red, the centrocone (MORN1) in black, β-tubulin in green, and the nucleus in gray. The cell division cycle progresses from left to right (a to d). (D) The kinetochore complex corotates to the basal end of nucleus upon spindle assembly. Wild-type parasites were costained with β-tubulin and TgNuf2 antisera to highlight the assembled spindle and the kinetochore, respectively. (E) The plastid remains at the top of the nucleus, and the spindle assembles at the basal end of nucleus. Wild-type parasites were costained with β-tubulin antiserum and Alexa 594–conjugated streptavidin to mark the assembled spindle and the plastid, respectively. β-Tubulin staining is shown in green, and other markers are shown in red. Bar, 3 μm.

tubulin relative to total β-tubulin in premitotic cells. Among all parasites with β-tubulin assembled at the centrocone (Figure 2B; counted population highlighted in green, purple, and blue blocks corresponding to the pie chart), 23% showed tubulin at the basal end alone, 38% showed tubulin at the apical end alone, 38% showed colocalization of acetylated α-tubulin and total tubulin at the apical end of nucleus, but only 1% showed basal localization. Hence we concluded that acetylation of α-tubulin occurs at the apical spindle MTs, and the 1% of basal-assembled acetylated spindles belong to the mispositioned centrosome/centrocone as reported in Morlon-Guyot *et al.* (2014).

These dynamics suggests that α-tubulin acetylation is involved in spindle stability, thereby regulating spindle assembly and disassembly. To test this model, we treated parasites with the histone

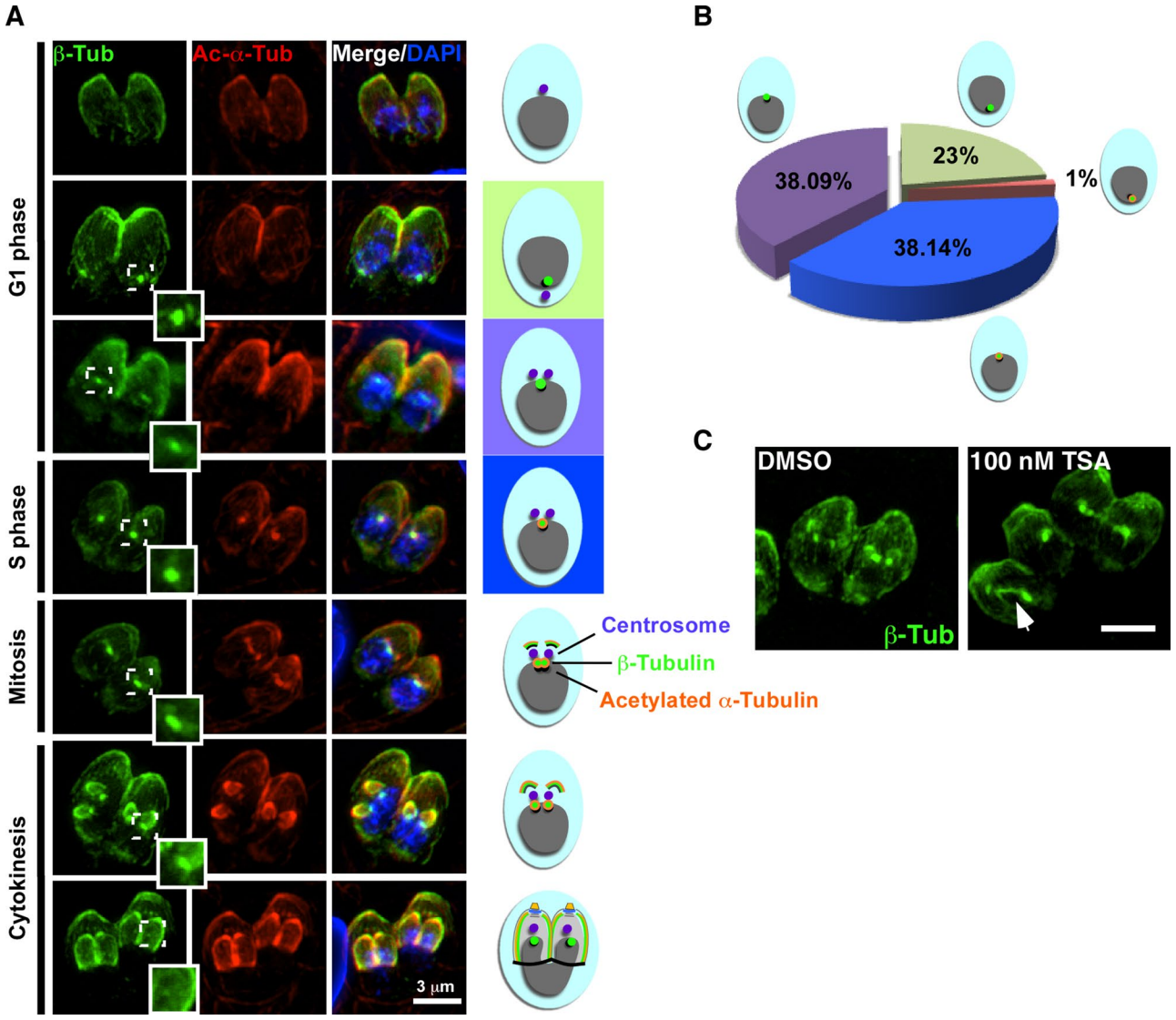

FIGURE 2: Acetylation of α-tubulin stabilizes spindle MT. (A) Acetylation of α-tubulin increases when the spindle rotates back to the apical end of the nucleus and is reduced before spindle disassembly. Costaining of wild-type parasites with β-tubulin (in green) and Ac-α-tubulin antibodies (in red). The insets highlight the spindle assembly. The cell cycle progression is shown from top to bottom and summarized by the schematic, in which the centrosome is shown in purple, the centrocone (MORN1) in black, β-tubulin in green, Ac-α-tubulin in orange, and the nucleus in gray. The colored background of the premitotic cells of schematics at rows 2–4 corresponds to the stage of quantified tubulin positioning and modification in the pie chart to the right. (B) Determination of the timing of spindle acetylation in mitotic cells (defined by the presence of nuclear β-tubulin). Intracellular parasites are stained as described for A. The incidence at which parasites displayed β-tubulin and Ac-α-tubulin distribution were scored in the four categories illustrated with the cartoons. The schematic represents the centrosome in purple, β-tubulin in green, and acetylation of α-tubulin in orange. (C) Inhibition of deacetylation promotes formation of aberrant spindle bundle. Wild-type parasites were treated with 100 nM TSA and stained with β-tubulin antiserum. The white arrow marks the spindle bundle MT. Bar, 3 μm.

deacetylase (HDAC) inhibitor trichostatin A (TSA), which has been shown to block TgHDAC-mediated histone deacetylation (Strobl *et al.*, 2007) and in other systems has been shown to also deacetylate MTs (Hubbert *et al.*, 2002). After TSA treatment, we observed aberrant spindle morphology: the segregated spindle poles are connected by an elongated tubulin structure, the result of stabilized, possibly bundled, spindle MTs (Figure 2C, white arrowhead). In conclusion, the spindle MTs assemble at the basal end of the nucleus, acetylation of α-tubulin follows spindle MT assembly, and acetylation of α-tubulin regulates stability of the spindle MTs. These observations suggest that the posttranslational modification of α-tubulin is involved in dynamic assembly and disassembly of spindle microtubules.

TgEB1 localizes to dynamic *Toxoplasma* MTs

To better characterize the dynamics of the mitotic spindle in *T. gondii*, we sought to identify MT-binding proteins specifically associated with spindle MTs during mitosis, as the α- and β-tubulin reagent reactivity with the subpellicular MTs surrounding the parasite obscures the spindle. We focused on the *Toxoplasma* orthologue

of a conserved MT plus end–binding protein EB1 acting on mitotic MT stability in other systems (Beinhauer *et al.*, 1997; Bu and Su, 2001; Komaki *et al.*, 2010). We BLAST searched ToxoDB using *Homo sapiens* (AAC09471.1) and *Chlamydomonas reinhardtii* (AAO62368.1) EB1 protein sequences and identified a single orthologous gene, TgEB1 (TGGT1_227650). The greatest conservation between apicomplexan EB1 and other eukaryotic EB1 proteins was observed in the CH domain, especially concentrated in the α-helixes of this domain (Figure 3A and Supplemental Figure S1). Four residues in direct contact with tubulin in the MT (Y84, L91, K104, and Q117) as defined in the *Schizosaccharomyces pombe* EB1 orthologue Mal3 (Maurer *et al.*, 2012) are conserved in TgEB1 (Figure 3A).

To define TgEB1 localization in *Toxoplasma*, we tagged the endogenous locus with a C-terminal yellow fluorescent protein (YFP). We monitored its subcellular localization throughout the cell division cycle in conjunction with mCherryRFP-tagged MORN1 as a centrocone and development marker. Throughout G1 phase, TgEB1-YFP was weakly but evenly distributed in the nucleoplasm, but upon onset of mitosis, TgEB1-YFP became concentrated in the centrocone, where it remained until completion of cytokinesis (Figure 3B). After separation of the spindle poles, TgEB1-YFP highlighted fiber-like structures emanating from the centrocones into the nucleoplasm (Figure 3B, arrowhead). We resolved this structure further using structured illumination microscopy and found that these fibers likely represent interpolar spindle MTs remaining after completion of mitosis (Figure 3C, arrowhead). We were unable to visualize these fibers with either tubulin antiserum (which has been responsible for the paucity of data on the *Toxoplasma* spindle), although these MTs have been observed in ultrastructural studies in apicomplexan parasites (Dubremetz, 1973; Morrissette and Sibley, 2002) and were easily visualized by immunofluorescence assay (IFA) in the related parasite *Sarcocystis neurona* (Vaishnava *et al.*, 2005). The use of TgEB1-YFP as a powerful spindle pole and spindle MT marker allowed us to establish the organization and assembly of the *Toxoplasma* mitotic apparatus.

We also observed TgEB1 labeling at the growing end of daughter cells, presumably the growing tips of the daughter subpellicular MTs right after completion of nuclear partitioning into the elongating daughter cells (Figure 3D, arrowheads). This localization pattern was not seen before encapsulation of DNA by the daughter cells (Figure 3D, top). This timing coincides with the halt in further extension of the subpellicular microtubules (Gubbels *et al.*, 2006; Anderson-White *et al.*, 2012) and highlights the presence of a potential regulatory switch associated with completion of nuclear partitioning and/or karyokinesis. Taking the results together indicates that TgEB1 generally localizes to the nucleoplasm in interphase, primarily interacts with the spindle microtubules, and briefly associates with the tip of the subpellicular MTs at the end of karyokinesis.

A C-terminal nuclear localization signal directs TgEB1 nuclear localization

The nucleoplasmic localization of TgEB1 led us to explore the presence of a nuclear localization signal (NLS) in TgEB1. It has been reported that the EB1c variant of *Arabidopsis thaliana* resides in the nucleoplasm mediated by a C-terminal extension of AtEB1c harboring two short basic-residue-containing NLS motifs (Komaki *et al.*, 2010). Protein alignment of TgEB1, AtEB1c, and MmEB1 showed that these basic-residue-containing motifs are not positionally conserved in TgEB1, and MmEB1 lacks the C-terminal extension (Figure 4A). We subjected TgEB1 to NLS finder programs and identified a basic residue-rich NLS within the last 23 amino acids (Figure 4A). To test whether this predicted NLS confers nuclear localization to TgEB1, we constructed a deletion mutant in which the last 23 amino acids are missing and fused it to YFP (TgEB1-ΔC^{23}-YFP). As shown in Figure 4B, nuclear localization was not affected by this deletion.

To functionally dissect the molecular nature of TgEB1 nuclear localization, we next focused on the unique N-terminal extension compared with other EB1 sequences (Figure 4A and Supplemental Figure S1B). Although these first 15 amino acids contain a few basic residues (H5 and R12), it is possible that TgEB1 enters the nucleus through association with another protein functioning as an escorter. TgEB1-ΔN^{15}-YFP localized to the nucleoplasm without any problems, so this section does not contain the NLS (Figure 4C). Finally, we expanded our focus to the unique C-terminus not shared with other EB1 sequences and noticed that this region contains several additional basic residues (Figure 4A), which could be part of a fragmented NLS. To test this possibility, we deleted the last 58 amino acids. During interphase, TgEB1-ΔC^{58}-YFP is present in the cytoplasm and no longer localizes to the nucleoplasm (Figure 4D). In some parasites, we do observe TgEB1-ΔC^{58} -YFP association with the subpellicular MTs (Figure 4D, top). However, TgEB1-ΔC^{58}-YFP remains associated with the spindle pole. It is possible that this pool of EB1 protein binds to the cytoplasmic side of the spindle MTs embedded in the centrocone, which is technically in contact with the cytoplasm, as the spindle pole resides in a fold of the nuclear envelope. Taken together, our data show that the C-terminal extension of TgEB1 harbors a NLS that endows TgEB1 with distinct compartmentalized behavior.

TgEB1 mutants alter spindle MT stability

The observation that TgEB1 localized to the whole length of the spindle MT (Figure 3C) was counterintuitive, as this appears to extend beyond the plus end. One possible explanation is scale, since the plus end can be up to 3 μm long in mammalian cells (Bieling *et al.*, 2007), which exceeds the diameter of the *Toxoplasma* nucleus. In general, EB1 association with the plus end is defined by the GTP-bound tubulin state at the plus end, whereas in the MT lattice, tubulin is in the GDP-bound state (Maurer *et al.*, 2012). Of interest, the affinity can be modulated by introducing mutations in the EB1 residues interacting with tubulin, as has been shown in *S. pombe* (Maurer *et al.*, 2012). With these mutations as a guide, we probed the interaction of TgEB1 with MTs with the goal of understanding TgEB1's affinity for MTs.

First, we tested the Q117E mutation, which should completely abolish affinity for MTs (Maurer *et al.*, 2012). We introduced TgEB1^{Q117E} as an exogenous allele fused to YFP into parasites already stably expressing mCherryRFP-MORN1. Overexpressed TgEB1^{Q117E}-YFP localizes to nucleoplasm throughout the cell cycle, with a concentration in the centrocone during mitosis (Figure 5A). This suggests that the Q117E mutation reduces, but does not abolish, the MT-binding affinity of TgEB1. However, the unexpected concentration of TgEB1^{Q117E}-YFP at the spindle poles could be mediated by dimerization of the mutant proteins with wild-type TgEB1 or, alternatively, could be due to MT-independent association at the centrocone. Moreover, we never observed labeling of the spindle MTs emanating into the nucleoplasm in parasites expressing TgEB1^{Q117E}-YFP, suggesting that the affinity for these MTs is greatly reduced, if at all present.

Second, we tested the Q117A mutation, which is expected to enhance MT binding and shift EB1 localization from the plus end to the entire MT lattice (Maurer *et al.*, 2012). TgEB1^{Q117A}-YFP

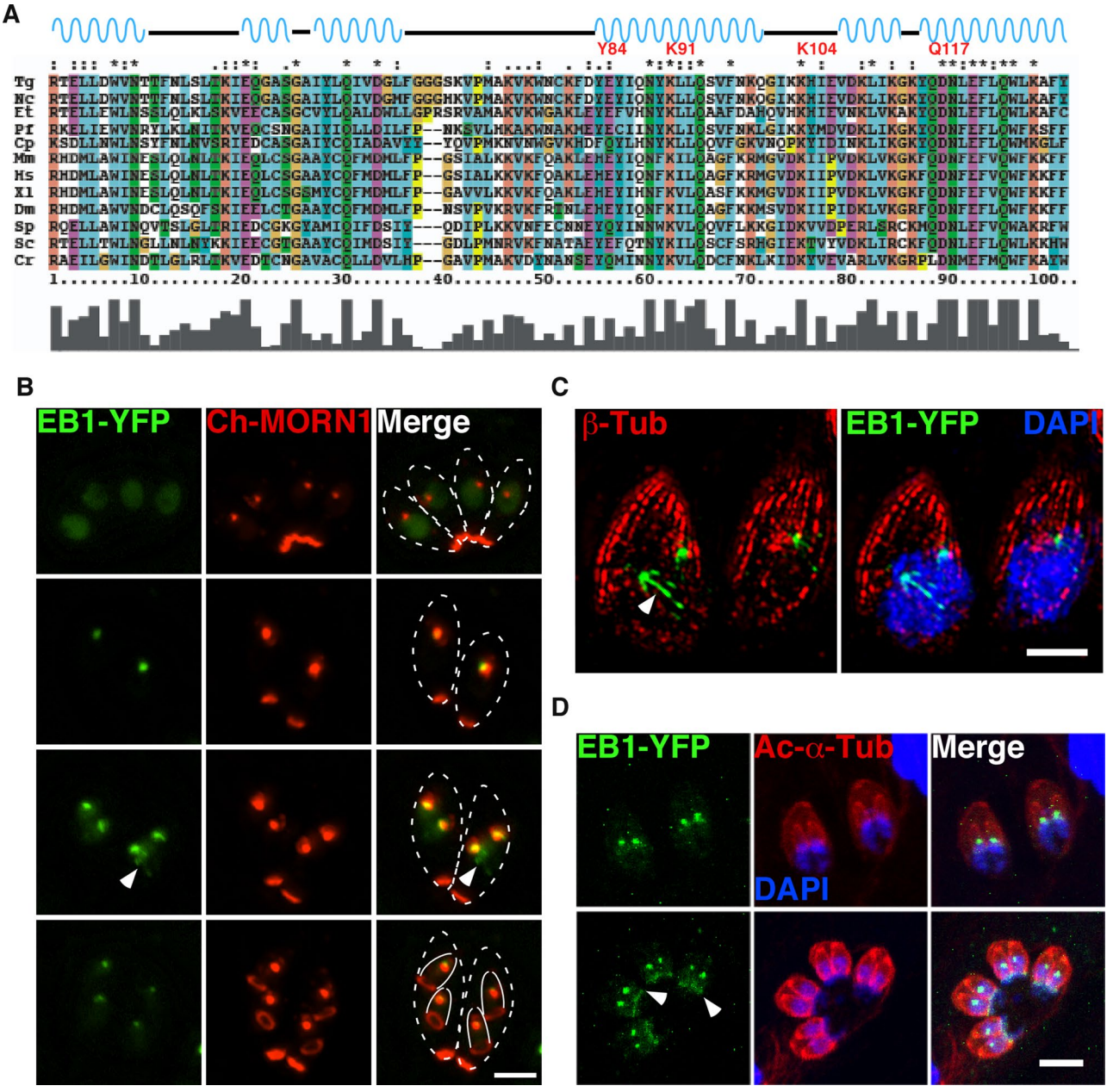

FIGURE 3: Identification and characterization of TgEB1. (A) Sequence alignment of EB1 CH domain of selected orthologues (*T. gondii* TGGT1_227650; *Neospora caninum* NCLIV_045630; *Plasmodium falciparum* PF3D7_0307300; *Eimeria tenella* ETH_00010720; *Homo sapiens* AAC09471; *Drosophila melanogaster* AAM70826.1; *Saccharomyces cerevisiae* AAB64549.1; *S. pombe* SPAC18G6.15; *Cryptosporidium parvum* cgd7_2370; *M. musculus* 13589; *Chlamydomonas reinhardtii* AAO62368.1; *X. laevis* 398293). The secondary structure is indicated at the top (blue wave represents α-helices), and the four conserved MT-interacting residues are marked in red (number represents the *Toxoplasma* residue number). The dark gray bars below the sequence alignment represent the conservation of the consensus sequence. Complete sequence alignment is shown in Supplemental Figure S1A. Protein modeling of TgEB1 on the HsEB3 crystal structure is shown in Supplemental Figure S4. (B) Dynamic localization of endogenously tagged TgEB1-YFP at the nucleoplasm, spindle pole, and spindle MTs. TgEB1-YFP–expressing parasites were stably cotransfected with an mCherryRFP-MORN1 construct as a developmental marker. Dashed white lines outline the mother parasite; solid white lines outline the daughter buds. The cell division cycle progresses from top to bottom. (C) TgEB1-YFP highlights the spindle MT protruding into the nucleoplasm (white arrowhead). Endogenously tagged TgEB1-YFP parasites were costained with β-tubulin antiserum and DAPI and analyzed by structured illumination microscopy. (D) TgEB1-YFP translocates to the growing end of daughter cells upon partitioning of divided nuclei into daughter cells. Endogenously tagged TgEB1-YFP parasites were costained with Ac-α-tubulin antibodies and DAPI. Arrowheads mark the YFP signal at the basal end of the daughter buds. TgEB1-YFP signals are shown in green and other markers in red. Bar, 3 μm.

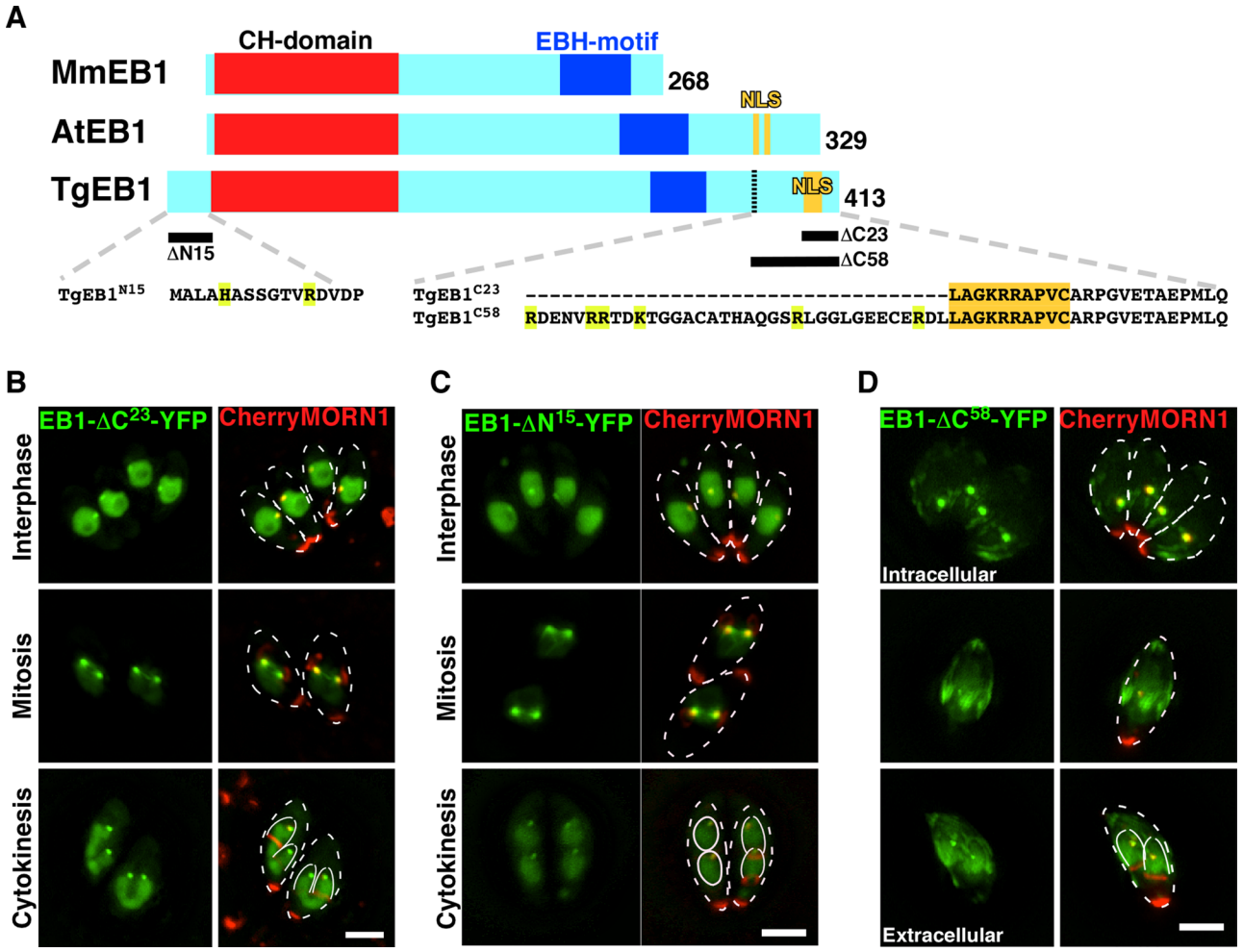

FIGURE 4: Mapping the TgEB1 nuclear localization signal. (A) Comparative domain analysis of mouse (Mm), *Arabidopsis thaliana* (At), and *T. gondii* EB1. MT-interacting CH domain is marked in red, EB1-homology motif in blue, and predicted NLS in yellow (we used both SeqNLS [http://mleg.cse.sc.edu/seqNLS/; Lin *et al.*, 2012] and cNLSmapper [http://nls-mapper.iab.keio.ac.jp/cgi-bin/NLS_Mapper_form.cgi; Kosugi *et al.*, 2009]). Black bars indicate the deleted amino acid region of TgEB1 truncation mutants ΔN^{15}, ΔC^{23}, and ΔC^{58}. The sequences of ΔN^{15} and ΔC^{58} are indicated. (B–D) Distinct localization patterns of TgEB1 truncation mutants. Parasites stably expressing mCherryRFP-MORN1 were transiently cotransfected with TgEB1-ΔC^{23}-YFP (B), TgEB1-ΔN^{15}-YFP (C), or TgEB1-ΔC^{58}-YFP (D). Cell division cycle stages are indicated on the left (B, C). White dashed lines outline the parasite; solid white lines mark budding daughter cells. Bar, 3 μm.

expression resulted in the appearance of elongated, bar-like structures of differing length and shapes extending throughout the nucleus (Figure 5B). These results suggest that expression of TgEB1^{Q117A}-YFP induces bundling of spindle MTs. We further analyzed the abnormal bar-like structures in TgEB1^{Q117A}-YFP–expressing parasites by immunofluorescence labeling of tubulin, which confirms that the bars are composed of tubulin and likely represent bundled MTs (Figure 5, C and D).

The 14 chromosomes of *T. gondii* tachyzoites remain clustered at the centromere throughout the division cycle (Brooks *et al.*, 2011; Farrell and Gubbels, 2014). To assess whether the TgEB1^{Q117A}-YFP–mediated spindle MT stabilization affects the kinetochore clustering and/or the interaction between the mitotic spindle and the chromosomes, we costained the parasites expressing TgEB1^{Q11A}-YFP with antisera for kinetochore and centromere markers TgNdc80 and CENP-A, respectively (Brooks *et al.*, 2011; Farrell and Gubbels, 2014). As shown in Figure 5, E and F, both markers resulted in a "beads on a string" pattern, with beads of variable size and intensity along the MT bundle. This suggests that the clusters of 14 centromeres, including their kinetochores, have been broken up into several smaller clusters representing <14 chromosomes. This implies that interaction of the kinetochore with the MT is stronger than the tethering force between the centromeres and/or kinetochores. Although the abnormal MT bundle disrupts the kinetochore complex, the structure of centrosome remains intact, as shown in Figure 5, G and H. It is tempting to hypothesize that the MT bundle is formed from the interpolar-MT bar assembled during the S/M transition (Figure 2A, S phase and mitosis). Increase of the MT-binding affinity of the TgEB1^{Q11A}-YFP mutant not only promotes the formation of the MT bundle, but also prevents it from disassembly, resulting in a long extension of the MT bundle.

To further examine the nature of the MT bundles and determine whether they penetrate into the cytoplasm, we performed transmission electron microscopy (TEM). In wild-type parasites, the

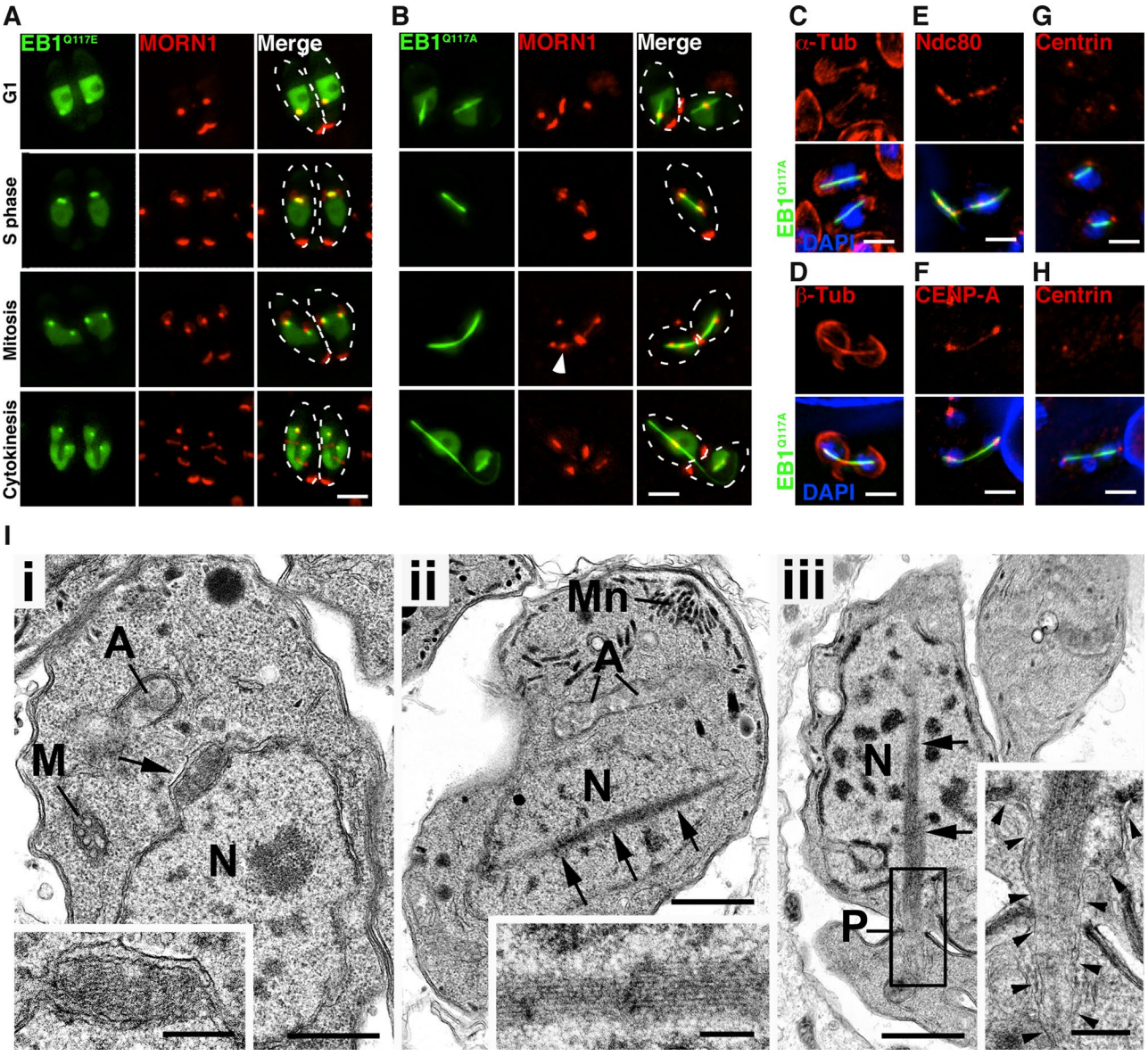

FIGURE 5: EB1 mutants display distinct MT-interacting affinity. (A) TgEB1^{Q117E}-YFP reduces affinity to the nuclear spindle MTs. Parasites stably expressing mCherryRFP-MORN1 were transiently cotransfected with a TgEB1^{Q117E}-YFP–expressing construct and imaged live 24 h posttransfection. Dashed white lines outline the parasites. The cell division cycle progresses from top to bottom, and phases are as indicated on the left (B) TgEB1^{Q117A}-YFP promotes formation of an abnormal bar-like structure. Parasites stably expressing mCherryRFP-MORN1 were transiently cotransfected with a TgEB1^{Q117A}-YFP–expressing construct and imaged live 24 h posttransfection. White arrowhead indicates the ruptured centrocone. (C–H) Wild-type parasites were transiently transfected with a TgEB1^{Q117A}-YFP–expressing construct and fixed 24 h after transfection. Parasites are stained with antisera against α-tubulin (C), β-tubulin (D), Ndc80 (E), CENP-A (F), and centrin (G, H). (C, D) The aberrant bar is composed of microtubules. (E, F) The aberrant bar disrupts clustered kinetochore complex. (G, H) The aberrant bar is bundled in between centrosomes. Bars, 3 μm. (I) Transmission electron microscopy of wild-type (i) and TgEB1^{Q117A}-YFP–expressing parasites (ii, iii). Bars, 500 nm (main images), 100 nm (insets). (i) WT parasite, illustrating the nucleus (N) with the small eccentric spindle (arrow). Inset, enlargement of the nuclear spindle, showing that it is enclosed by the nuclear membranes. A, apicoplast; M, mitochondrion. (ii) TgEB1^{Q117A}-YFP parasite exhibiting a rod-like structure (arrows) running through the nucleus (N). Inset, enlargement of the rod, showing the tightly packed microtubules lying naked in the nucleoplasm. A, apicoplast; Mn, micronemes. (iii) Mutant parasite showing the rod-like structure (arrows) running through the nucleus (N) and extending into the cytoplasm, passing through a posterior pore-like structure (P). Inset, enlargement of the enclosed area, showing the nuclear membranes extending over the protruding rod (arrowheads).

polar spindle MTs are short and assembled eccentrically into a tunnel-like space embedded in the nuclear membrane (Figure 5Ii, arrow and inset), as reported previously (Ferguson and Dubremetz, 2013). In contrast, in the Q117A mutant, the MTs are significantly longer and form a tightly packed, rod-like structure that is in direct contact with the nucleoplasm with no surrounding membrane (Figure 5Iii, arrow and inset). However, when the packed, rod-like MT bundle is examined for possible penetration into the cytoplasm

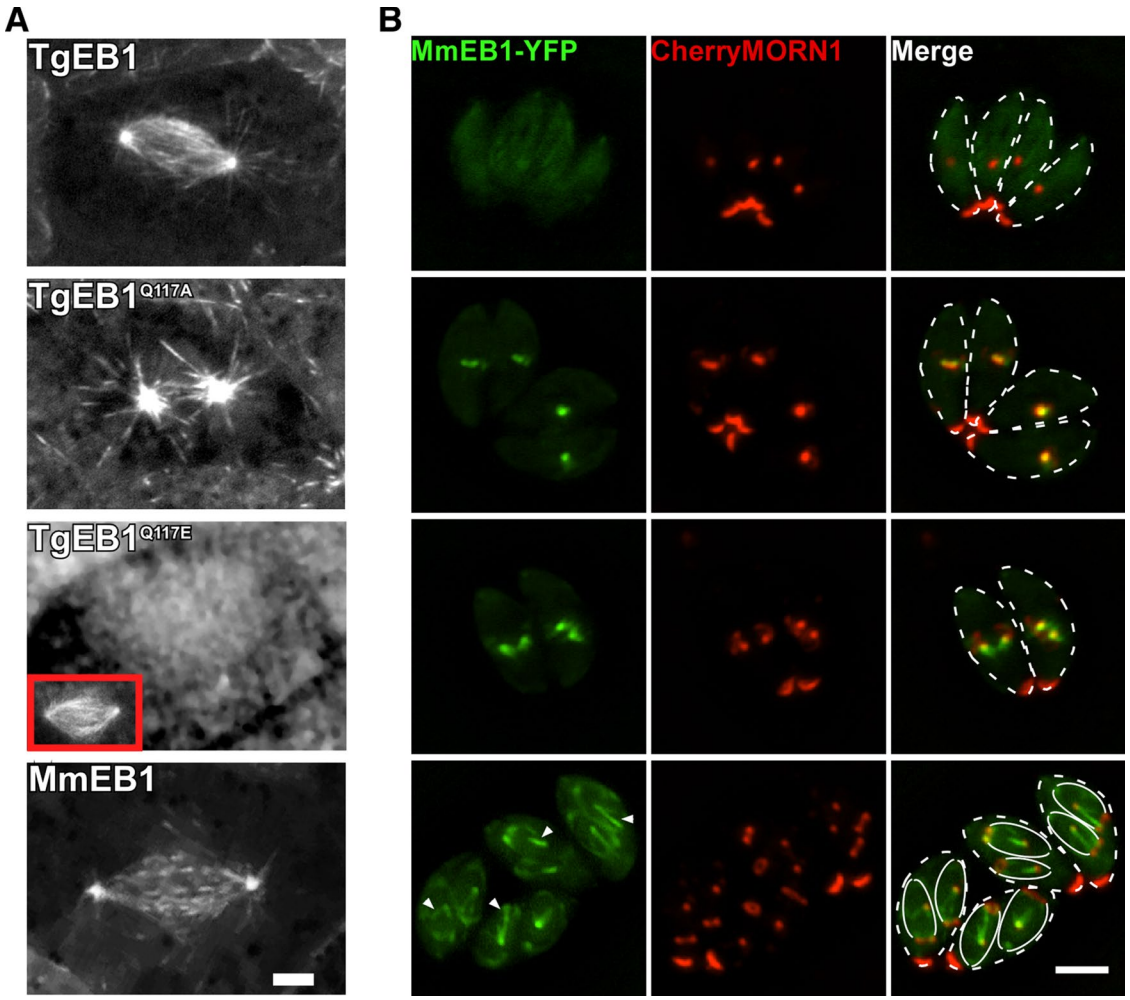

FIGURE 6: Comparative behavior of vertebrate and *Toxoplasma* EB1 proteins by reciprocal expression in *T. gondii* tachyzoites and in *Xenopus* embryos. (A) Still images of *Xenopus* mitotic epidermal cells transiently expressing TgEB1-YFP, TgEB1^{Q117A}-YFP, TgEB1^{Q117E}-YFP, and mouse (*M. musculus*) MmEB1-YFP. The red box represents the mitotic spindle in the same cell labeled by MmEB1-mKate2 as a control for intact spindle assembly. The complete data set is given in Supplemental Figure S3; complete time-lapse movies are provided in Supplemental Movies S1–S3 (scale bar, 5 µm). (B) Dynamic localization of MmEB1-YFP in *T. gondii*. Transient expression of mouse MmEB1-YFP in *T. gondii* tachyzoites stably expressing mCherryRFP-MORN1. Note the general exclusion from the nucleus (scale bar, 3 µm). Dashed and solid white lines outline mother parasites and daughter buds, respectively. Arrowhead marks the spindle MTs emanating from the spindle pole.

by TEM (Figure 5B), it appeared that the portion of the spindle protruding into the cytoplasm is enclosed by an extension of the nuclear membrane (Figure 5Iiii, arrowhead and inset). In addition to the changed dynamics of the nuclear membranes, the other key observation is that the elongated structure is indeed consistent with bundled MTs. Taken together, our data show that the conserved Q117 is crucial for the MT-binding affinity of TgEB1. Overexpression of TgEB1^{Q117A}-YFP stabilizes MT bundles and promotes formation of aberrantly long MT bundles, which disrupts the otherwise stable centromere/kinetochore clustering.

TgEB1 dynamics mimics vertebrate EB1 in different vertebrate cell types

As mentioned, we observed that the entire length of MTs in the *Toxoplasma* nucleoplasm is coated with EB1 (Figure 3, B and C). This may be due to a high local concentration of EB1 in the nucleus or to the relatively short length of these MTs. However, the observation that TgEB1^{Q117A} induces formation of MT bundles led us to consider whether the affinity of TgEB1 for MT differs from that of orthologous proteins in other eukaryotes. To test this possibility, we expressed TgEB1 in vertebrate cells and also reciprocally introduced a vertebrate EB1 in *Toxoplasma*. We expressed wild-type TgEB1-YFP, as well as the Q117A and Q117E mutants, in *Xenopus laevis* embryos and compared their behavior to that of mouse EB1 (*Mus musculus*; MmEB1), which is well understood (Lowery *et al.*, 2013). Because EB1 behavior depends to some extent on the MT type, we examined a combination of mitotic epidermal cells, interphase neuronal growth cones, and interphase neural crest cells from *Xenopus* embryos. Localization of wild-type TgEB1 was indistinguishable from that of MmEB1 in all three cell types (Figure 6A, Supplemental Figure S2, and Supplemental Movies S1–S3). As expected, TgEB1^{Q117E} completely lost affinity for MTs in all cell types (we identified the spindle in epidermal cells by coexpression of a mammalian EB1 tagged with mKate2 fluorescent protein along with TgEB1^{Q117E}-YFP; red box in Figure 6A and Supplemental Figure S2). For TgEB1^{Q117A}-YFP, we observe differences per cell type: plus-end

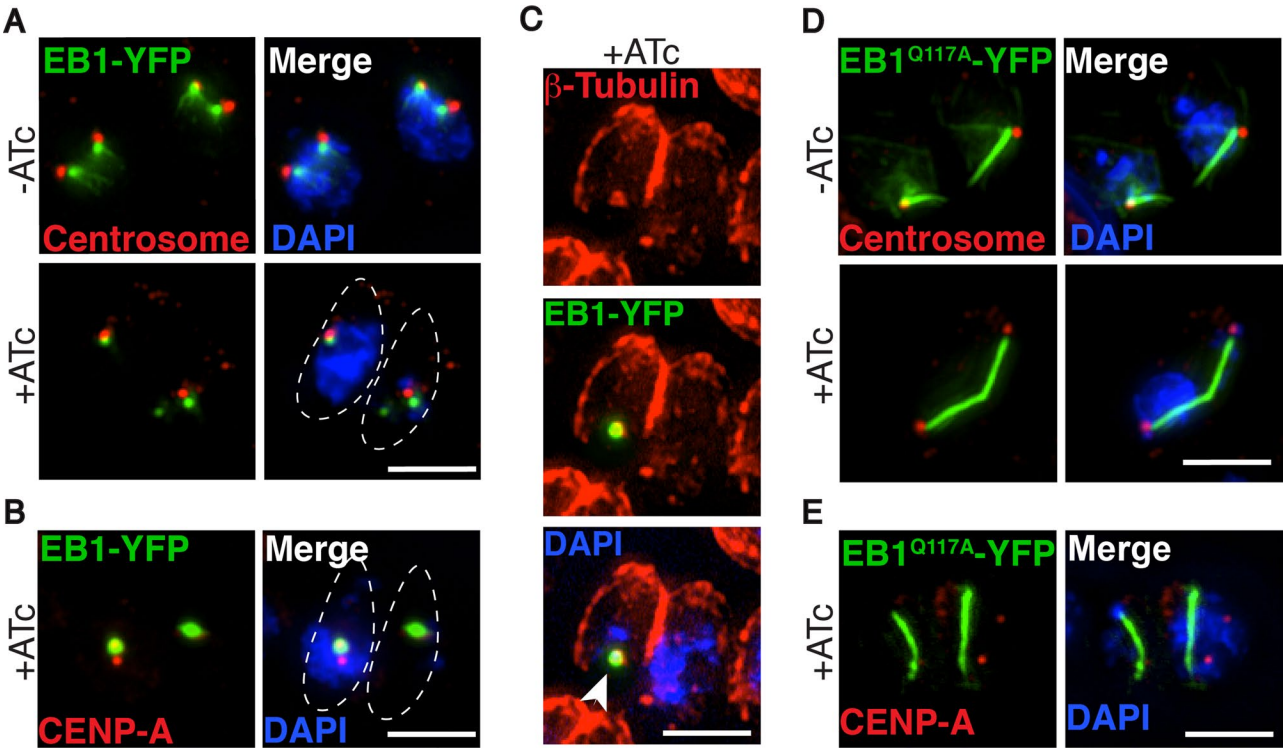

FIGURE 7: Fate of the spindle in absence of the Ndc80 complex. TgEB1-YFP constructs were transiently transfected into the TgNuf2-cKD parasite line, seeded into HFF cells, and analyzed with and without ATc for 12 h. Dashed white lines outline the parasites (scale bar, 3 μm). (A, B) TgEB1^{WT}-YFP remains associated with the centrosome in the absence of TgNuf2. TgEB1^{WT}-YFP costained with either Centrin to mark the centrosome (A) or CENP-A antisera to mark the centromeres (B). (C) TgEB1^{WT}-YFP associates with spindle MTs, indicated by costained β-tubulin antiserum. The white arrowhead marks the remnant of the centrocone (spindle pole) in an anucleate cell. (D, E) TgEB1^{Q117A}-YFP–induced MT bundles failed to rescue chromosome segregation defects in the absence of TgNuf2. TgEB1^{Q117A}-YFP costained with either HsCentrin to mark the centrosome (D) or CENP-A antiserum to mark the centromeres (E). Bar, 3 μm.

localization in growth cones, enhanced MT lattice affinity lattice in interphase neural crest cells, and spindle MT association comparable to that in wild-type TgEB1 and MmEB1. The behavior in interphase cells is consistent with our observation of enhanced MT-binding affinity caused by the Q117 mutation (Figure 5), but we never see induction of MT bundling in *Xenopus* cells. Overall TgEB1 behavior closely mimics that of MmEB1 in *Xenopus* cells, whereas formation of MT bundles promoted by TgEB1-^{Q117A} in *Toxoplasma* is possibly due specific conditions in the *Toxoplasma* system. Therefore the apparent increase in MT affinity seems to be caused by inherent features of the *Toxoplasma* system.

For the reciprocal experiment, we assessed the dynamics of MmEB1 in *Toxoplasma*. During mitosis, MmEB1-YFP interacts with the spindle pole and mitotic spindle in *T. gondii*, and also it associates with the subpellicular MTs of interphase and budding daughter cells (Figure 6B, top). Basically, during mitosis and cytokinesis, TgEB1 and MmEB1 display almost identical dynamics: MmEB1-YFP was recruited to the spindle pole and mitotic spindles (Figure 6B, arrowhead) and accumulated at the growing end of elongated daughter cells (Figure 6B, bottom). This is in contrast to interphase, when MmEB1-YFP is present in the whole cytoplasm and, unlike TgEB1, is excluded from the nucleus. We reasoned that since vertebrate mitosis occurs after nuclear envelope breakdown, MmEB1 does not need to be inside the nucleus. Overall our results suggest that TgEB1 generally functions similarly to vertebrate EB1 but has privileged nuclear access during closed mitosis and that the distinct effects on *Toxoplasma* are likely caused by factors other than TgEB1 in the *Toxoplasma* system.

TgEB1 stabilizes spindle MTs in absence of the Ndc80 complex

We previously showed that the Ndc80 complex is essential for *Toxoplasma* mitosis (Farrell and Gubbels, 2014). In those experiments, we used a parasite line in which Nuf2 expression is under the control of an anhydrotetracycline (ATc)-regulatable promoter. We established that loss of Nuf2 caused dissociation of the nucleus from the centrosome with the consequent formation of anucleate cells. Our new TgEB1 reagents permit the assessment of the fate of spindle MTs in the Nuf2 mutant. Furthermore, we speculated that stabilization of the spindle MTs might be able to rescue the loss of Nuf2 if other kinetochore protein complexes, such as a functional orthologue of KNL1 found in other eukaryotes (Kline-Smith *et al.*, 2005), could interact with the MTs. Thus we expressed YFP-tagged TgEB1, either the wild type or the Q117A allele, and subsequently repressed Nuf2 expression. We then analyzed the development of TgEB1-bound MTs, centrosomes, and centromeres. As shown in Figure 7A, in the absence of Nuf2, TgEB1-YFP remains associated with the centrosome, which is partitioned normally into the anucleate daughter cell (Figure 7A, +ATc). However, both centromere clusters remain in the undivided nucleus in the other daughter, where only one cluster appears to be associated with the spindle MTs (Figure 7B). Labeling with tubulin antibodies indicates that TgEB1

colocalizes with tubulin in the anucleate cell, indicating that it associates with MTs in the absence of the kinetochores (Figure 7C, white arrow). Of interest, TgEB1 is no longer associated in the other daughter, indicating that the cell cycle progressed into interphase; this suggests that the presence of a nucleus in the parasite is required to destabilize the spindle MTs.

Formation of MT bundles by expression of TgEB1^{Q117A}-YFP was equally unable to rescue the TgNuf2-knockdown phenotype (Figure 7, D and E). However, we clearly observe a MT bundle associated with the centrosomes (Figure 7D), indicating that the assembly of spindle MTs is possible in the absence of the Ndc80 complex. Furthermore, we observe that the centromeres are no longer associated with the bundled MTs and that the clusters have not fragmented (Figure 7E). This is consistent with the function of Nuf2 in mediating kinetochore MT interaction and further indicates there is no other major force (such as a functional orthologue of KNL1) acting on this interaction.

Because we were never able to detect spindle MT with the antisera reagents in the Nuf2 mutant (Farrell and Gubbels, 2014) our results suggest that overexpression of wild-type TgEB1 is already sufficient to bundle the spindle MT (Figure 7C). Indeed, high levels of wild-type EB1 protein promote the formation of MT bundles in distinct cell types (Beinhauer *et al.*, 1997; Schwartz *et al.*, 1997; Ligon *et al.*, 2003). Although we rarely observed formation of bundle MTs upon transient overexpression of wild-type TgEB1-YFP in the wild-type parasite background, we were unable to establish a parasite line stably transfected with this construct. This suggests that the level of TgEB1 is tightly regulated and is calibrated to timing and maintenance of the desired spindle MT dynamics.

Deletion of EB1 induces defects in parasite proliferation

To further dissect the function of TgEB1 we established a direct knockout line, TgEB1-KO, using clustered regularly interspaced short palindromic repeats (CRISPR)/Cas9-mediated genome editing (Shen *et al.*, 2014; Sidik *et al.*, 2014). We substituted the endogenous TgEB1-coding DNA with a 1.5-kb HXGPRT drug-selectable cassette flanked by 35–base pair homologous sequences to the CRISPR/Cas9-generated DNA breaks to facilitate site-specific double homologous recombination (Figure 8A). Diagnostic PCR confirmed the correct genotype of the TgEB1-KO line (Figure 8A, right). To examine the viability of TgEB1-KO parasites, we performed a plaque assay and found a modest, 33% reduction in plaque size (Figure 8B). To assess whether this reduction is due to replication defects, we performed IFAs on the TgEB1-KO line using a series of mitotic markers. Although the nonmitotic TgEB1-KO parasites appeared to have a normal morphology, 65% of mitotic parasites showed an unusual scattered kinetochore structure (Figure 8, C, inset, and E), sometimes resulting in a stray kinetochore (Figure 8C, white arrowhead). In these deviant TgEB1-KO cells, we found that the straggling kinetochores were observed only in anaphase cells and not in interphase cells (Figure 8D). The amount of scattered-kinetochore-containing cells in the mitotic TgEB1-KO line is five times higher than with the wild type (Figure 8E). However, the fact that plaque size is only modestly reduced and the vast majority of nonmitotic parasites appear normal suggests that the abnormal kinetochore structure caused by TgEB1 depletion was resolved well by the parasite but might result in a delay to complete mitosis and as such be responsible for the smaller plaques. In parallel, we also established a conditional knockdown line of 2xMyc-tagged TgEB1 (TgEB1-cKD; Supplemental Figure S3A). A similar scattered-kinetochore phenotype and modest growth defect were observed when TgEB1-2xMyc was depleted, confirming that in the absence of TgEB1, the parasite can cope with minor defects (Supplemental Figure S3). TgEB1-YFP remains in close proximity with the kinetochore marker Ndc80 throughout mitosis (Figure 8F). Thus we hypothesize that TgEB1 contributes to kinetochore clustering by either bundling the kinetochore MTs or maintaining equal length of the kinetochore MTs, and in the absence of TgEB1, the acting MT forces split the clustered kinetochores (Figure 8G). Combining these observations with the information on EB1^{Q117A} mutant observations, where kinetochores become unclustered as well, we conclude that TgEB1 plays a role in securing mitosis accuracy by controlling spindle dynamics.

DISCUSSION

Our analysis of the spindle MTs in *T. gondii* tachyzoites revealed that their formation and acetylation are tightly orchestrated with centrosome rotation (Figures 1 and 2). Spatially, this fits with the MTOC activity of the centrosome. Because the centrosome is the signaling hub in *Toxoplasma*, the mechanism underlying the timing of spindle MT assembly likely also resides in the centrosome. Although we previously showed that separation of duplicated centrosomes requires TgNek1 kinase activity (Chen and Gubbels, 2013), their physical partitioning relies on assembly of spindle MTs (Morrissette and Sibley, 2002; Farrell and Gubbels, 2014). More puzzling is the biological significance of centrosome rotation before duplication. It was previously postulated that rotation uncouples the centrosome from the apical organelles it organizes (such as the Golgi apparatus and apicoplast), permitting duplication in isolation (Hartmann *et al.*, 2006). That model is not supported by our data, as the centrosome appears to be anchored to the spindle pole, and likely the whole nucleus is rotated. It is possible the centrosome rotation plays a role in determining or establishing cell polarity before committing to cell division, a role that is well documented in many systems, such as *Drosophila* oocyte development (Megraw and Kaufman, 2000), fibroblast migration, T-cell–target interaction, syncytial muscle cell development, and neuron development (Li and Gundersen, 2008). Regarding *Toxoplasma*, it was recently shown that both myosin F (Jacot *et al.*, 2013) and CDPK7 (Morlon-Guyot *et al.*, 2014) affect centrosome positioning in the cell; the former has a dramatic effect due to polar positioning of centrosomes, resulting in fatal apicoplast division defects, whereas the latter results in centrosome partitioning and positioning defects but did not cause much detriment to development. It is possible that this mechanism is more relevant for schizogony, in which multiple daughters undergoing external budding require association with the plasma membrane, but is not as critical in *Toxoplasma*'s asexual binary division cycle, which undergoes internal budding.

We demonstrated that TgEB1 contributes to the organization of spindle MTs (Figures 3–8). The nearly exclusive association of TgEB1 with spindle MT was rather surprising because *T. gondii* tachyzoites contain distinct populations of MTs (stable conoid, subpellicular, and central apical pair MTs and dynamic spindle MTs), which have different polymerization and stability properties (Gubbels and Morrissette, 2013). The differential regulation of these diverse MT populations is not well understood. In part, this regulation can be attributed to unique MT-associated proteins binding to specific MT populations, as shown for subpellicular microtubule- associated proteins SPM1 and SPM2 (Tran *et al.*, 2012). Following this logic, TgEB1 appears to have a spindle-specific role.

We considered several models to explain the observation that the entire MT length is coated with TgEB1 rather than being restricted to the plus end. It has been shown that the affinity of EB1 for the plus end versus the entire lattice is moderated by the concentration of EB1 (Lee *et al.*, 2000; Bu and Su, 2001). The specific accumulation of TgEB1 in the nucleoplasm could indeed be associated with

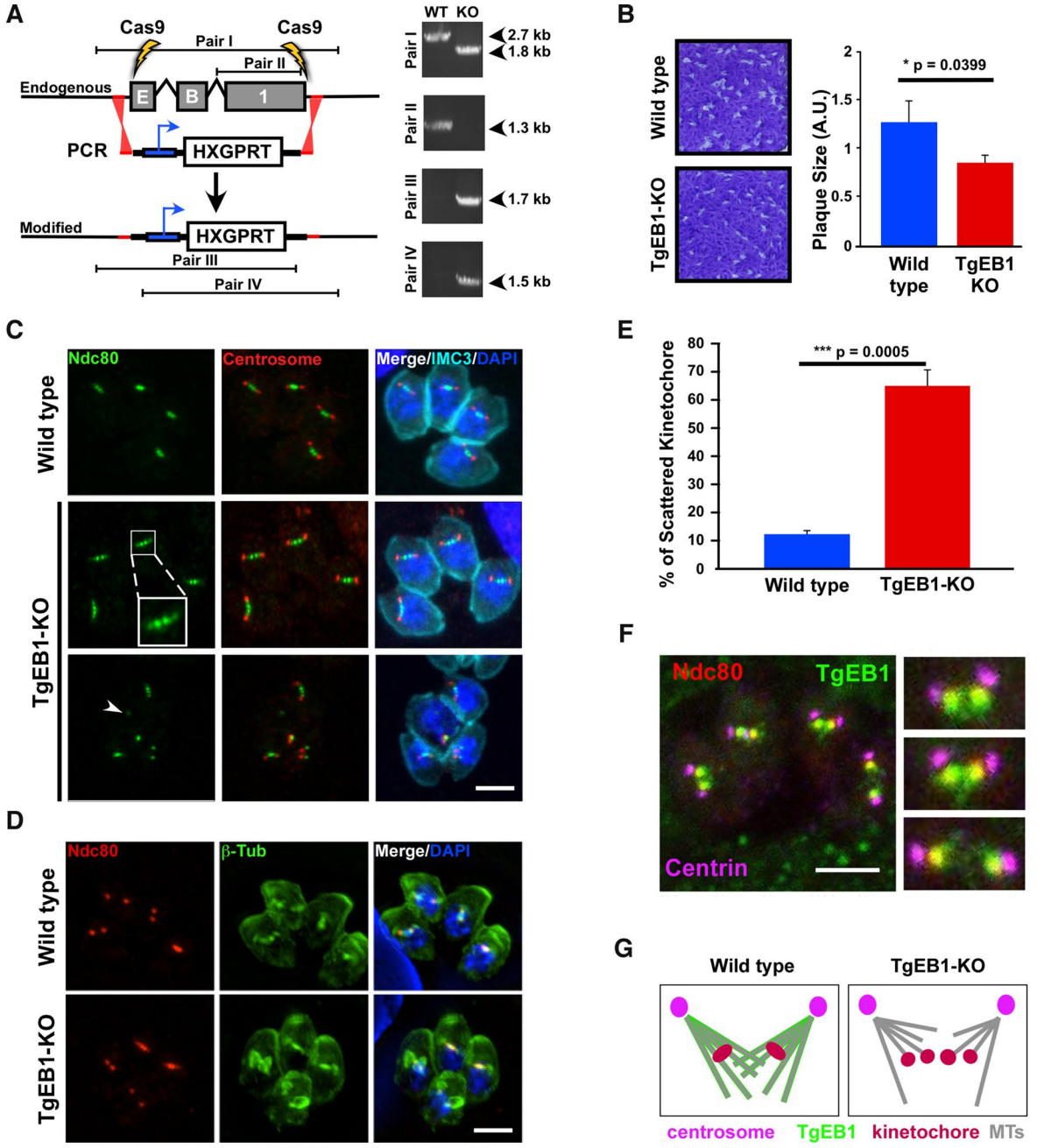

FIGURE 8: Knockout of TgEB1. (A) Schematic representation of TgEB1-KO transgenic line construction by CRISPR/Cas9-mediated homologous recombination. The position of two double-strand breaks created by Cas9 nuclease is marked by yellow lightning bolts. The red bars represent the 35 base pairs of 5′ and 3′ homologous regions flanking the break sites. Diagnostic PCR primer pairs I–III validating the replacement of the endogenous TgEB1 locus (marked by gray blocks) by the 1.5-kb PCR product containing the HXGPRT cassette are as indicated. Diagnostic PCRs of TgEB1-KO and its parental line using primer pairs I–III confirm the expected genotype. (B) Plaque assay of TgEB1-KO shows a reduction in plaque size compared with wild type after 7 d of incubation before fixation. Plaque size was measured from 50 plaques/sample in three independent experiments with an arbitrary unit by ImageJ (National Institutes of Health, Bethesda, MD) and analyzed with $p < 0.05$ (unpaired *t* test); error bars indicate SD. (C) IFA of wild-type and TgEB1-KO cells using α-Ndc80, α-Centrin, and α-IMC3 as kinetochore, centrosome, and parasite cytoskeleton markers, respectively. The inset magnifies the scattered kinetochores in the corresponding square; the white arrowhead marks a drifted kinetochore in an unequally segregated nucleus. (D) IFA shows that the scattered kinetochores appear in cells that underwent mitosis, using β-tubulin antiserum as a spindle MT marker. (E) Quantification of cells with the scattered-kinetochore phenotype. Up to 100 vacuoles with mitotic cells were counted from three independent experiments (total cell number, 336–352). Mitotic spindle staining using β-tubulin was used as a marker determining mitosis. $p < 0.01$ (Student's unpaired *t* test); error bars indicate SD. (F) TgEB1-YFP (green)–expressing parasites costained for the centrosome (in magenta) and kinetochore (in red) show that the kinetochore complex resides in close apposition to the TgEB1-YFP–highlighted spindle poles. (G) Model of spindle association with the kinetochore in the wild-type and TgEB1-KO lines. Centrosomes are shown in magenta, TgEB1 in green, kinetochores in red, and MTs in gray. Bar, 3 μm.

a locally elevated concentration. An observation conflicting with this model is that the spindle MTs are contained within a membrane-bound nuclear compartment as visible by TEM (Figure 5Ii; Gubbels *et al.*, 2006). This is further supported by the observation that TgEB1-ΔC^{58}-YFP does not enter the nucleoplasm and yet is still associated with the spindle (although it could potentially dimerize with wild-type TgEB1 and then reach the spindle pole). Furthermore, MmEB1, which lacks a C-terminal extension containing an NLS, when expressed in *Toxoplasma* tachyzoites, does not localize to the nucleoplasm but still associates with the spindle (Figure 6B). Collectively our data highlight that the nuclear spindle assembles in a privileged membranous compartment distinct from the nucleoplasm and cytoplasm, but experimental support for a locally higher concentration of TgEB1 is limited.

Second, we considered a potentially TgEB1-specific affinity for GDP-bound tubulin in the MT lattice versus GTP-bound tubulin at the plus end. We observed similar effects with the corresponding substitution of an MT-interacting residue in TgEB1 compared with the fission yeast orthologue, Mal3 (Iimori *et al.*, 2012; Maurer *et al.*, 2012). We hypothesize that the extended TgEB1^{Q117A}-YFP–bound MT bundle shown in Figure 5Iii, is formed from the early-assembled short-spindle MT (Figure 5Ii), and the increased affinity of TgEB1^{Q117A}-YFP prevents the bundled MT from breaking. Of note, hyperstabilized cytoplasmic and spindle MTs were observed with the orthologous mutation in *S. pombe* (Iimori *et al.*, 2012). Furthermore, it has been reported that overexpression of wild-type EB1 in other systems also induces increased MT stability and bundling (Beinhauer *et al.*, 1997; Schwartz *et al.*, 1997; Bu and Su, 2001; Ligon *et al.*, 2003). Wild-type TgEB1 and MmEB1 overexpression sporadically induces bundles in *Toxoplasma*, whereas TgEB1^{Q117A} overexpression induces bundle formation at a high frequency. Expression of TgEB1 in different vertebrate cells results in an indistinguishable MT interaction pattern from that for MmEB1 (Figure 6), suggesting that the bundle formation is not due to some unique properties inherent to TgEB1 itself but to other factors or modifications associated with spindle MT and/or TgEB1.

The level of nuclear localized TgEB1 is critical to its correct function, given that we were unable to obtain parasite lines stably expressing the wild-type, Q117E, or Q117A allele but obtained only stable transfectants for TgEB1-ΔC^{58} lacking the NLS. Thus it is possible that the nuclear saturation or constitutively expression of TgEB1 is lethal to the parasites. Alternatively, this may be due to dominant-negative depletion of interacting proteins with the simultaneously present endogenous TgEB1. In this context, we should also consider functions independent of MT binding. In this light, the current understanding of AtEB1c is relevant. AtEB1c is in the nucleus during interphase and is required for positioning of spindle poles and chromosome segregation; however, after disassembly of the nuclear envelope, AtEB1c translocates to the phragmoplast MTs during cytokinesis (Komaki *et al.*, 2010). Therefore the function of nuclear localization likely resides in spatiotemporal control of its activity such as the timing of events between mitosis and cytokinesis. As such, it is noteworthy that TgEB1 also associates with the subpellicular MTs late in cytokinesis. The timing coincides with completion of karyokinesis but before the disassembly of the spindle MTs. Thus we have identified the potential presence of such a switch in the spatiotemporal behavior of TgEB1, which will be the focus of future work.

The extended bundle formed by TgEB1^{Q117A}-YFP expression disrupts the clustering of the kinetochore complex and associated chromosomes (Figures 5, E, F, and H). Moreover, in the TgEB1-KO line the clustered kinetochore complex is also dispersed when the spindle poles segregate (Figure 8, C, E, and G). These results indicate that the interaction of the kinetochore with the MT is stronger than the tethering force between the centromeres and/or kinetochores and that TgEB1 may as such indirectly secure kinetochore clustering and promote accurate chromosome partitioning. In TgEB1-KO cells, we found ~10% of vacuole-containing cells with defective mitosis, including unequal segregation of DNA and DNA fragmentation, whereas in wild type, only 1.9% was observed (unpublished data). We reasoned that this small population of cells reflects the consequence of scattered kinetochores that may result in defective mitosis, since parasites receiving an aberrant copy of genetic material are likely unviable (Figure 8C and Supplemental Figure S3G). Alternatively, increase in cell cycle length due to prolonged mitosis could also contribute to the reduced plaque size in TgEB1-KO line. Collectively this shows that the main function of TgEB1 during mitosis is either the bundling of the spindle MTs or maintenance of an even length of the spindle MTs, which secures the correct segregation of the chromosome between the daughters. Given that EB1's role in other system is consistent with a bundling function, we favor the first model. In addition, these data consolidate our previous observations indicating that kinetochore clustering during mitosis is critically dependent on MT association, whereas during interphase, kinetochore clustering is independent of MTs (Farrell and Gubbels, 2014). Hence the mechanism of kinetochore clustering and centrocone association differs between interphase and mitosis.

Parasites lacking TgEB1 also displayed a minor cytokinetic defect, in particular in the completion of cell division (Supplemental Figure S3G). Defects in cytokinesis could be secondary effects due to problems with mitosis or could be linked with the association of TgEB1 with the ends of emerging daughter subpellicular MTs (Figure 3D), which is the model we favor. Overall we have characterized the dynamics of spindle MTs and identified a unique role for TgEB1 in *Toxoplasma* that functions in the novel regulatory mechanism not found in other eukaryotes.

MATERIALS AND METHODS

Parasites

T. gondii type I RH tachyzoites and their transgenic derivatives were grown in human foreskin fibroblasts (HFFs) as described in Roos *et al.* (1994). The following lines have been described before: RH::Δ*ku80* (Huynh and Carruthers, 2009) was kindly shared by Vern Carruthers (University of Michigan), TATi::Δ*ku80* (Sheiner *et al.*, 2011) was kindly shared by Boris Striepen (University of Georgia), and TgNuf2-cKD was generated by Farrell and Gubbels (2014). The TgEB1-KO line was established by replacing the endogenous locus with a 1.5-kb PCR product composed of an HXGPRT drug-selectable cassette and the TgEB1-cKD line with a 4.1-kb PCR product composed of DHFR-Tet7Sag4-TgEB1-(CDS)-2xMyc. Both PCR products were flanked by 35 base pairs of homologous sequence around 5′- and 3′-TgEB1 near the double-strain break generated by Cas9 nuclease. Two sets of single guide RNA targeting N- and C-termini of TgEB1 were used to induce site-specific DNA breaks to facilitate homologous recombination. All stably transfected lines were established by drug selection and cloned by limiting dilution.

Plasmids

All primer sequences used in this study are listed in Supplemental Table S1. YFP-tagged TgEB1, MmEB1, TgEB1 truncation mutants (TgEB1-ΔN^{15}, TgEB1-ΔC^{23}, and TgEB1-ΔC^{58}), and two mutant derivatives (TgEB1^{Q117A} and TgEB1^{Q117E}) were cloned in the *ptub*-YFP_2(MCS)/sagCAT plasmid (Anderson-White *et al.*, 2011). Both point mutants were created by megaprimer PCR mutagenesis (Lai *et al.*, 2003). The pU6 CRISPR/CAS9 plasmid was a kind gift

from Sebastian Lourido (Whitehead Institute), and genome editing using the CRISPR/CAS9 system was performed as described (Sidik *et al.*, 2014). Two pU6 CRISPR/CAS9 plasmids targeting different PMA sites of TgEB1 gene were generated (Figure 6A). TgEB1 and the mutant derivatives were cloned in the pCS2 *Xenopus* expression plasmid (Lowery *et al.*, 2013).

Immunofluorescence assay and light microscopy

IFAs were performed essentially as described in Gubbels *et al.* (2006) on 100% methanol–fixed parasites. The primary antibodies used in this study were as follows: β-tubulin (rabbit, 1:500; Morrissette and Sibley, 2002); acetylated α-tubulin (monoclonal antibody [mAb] 6-11B-1, mouse, 1:1000; Abcam); cMyc (mAb 9E10, mouse, 1:50; Santa Cruz Biotechnology); TgNuf2 (guinea pig, 1:2000; Farrell and Gubbels, 2014) and TgNdc80 (guinea pig, 1:2000; Farrell and Gubbels, 2014); SPM1 (mouse, 1:1000; Tran *et al.*, 2012); CENP-A (mAb, mouse, 1:20; Francia *et al.*, 2012; kindly shared by Boris Striepen); HsCentrin (rabbit, 1:1000; kindly shared by Iain Cheeseman, Whitehead Institute); and FLAG (rat, 1:200; Sigma-Aldrich). Alexa Fluor 488, 568, 594, and 633 goat anti-mouse, anti-rabbit, and anti–guinea pig secondary antibodies were used, as well as A594-conjugated streptavidin for the plastid (1:500; Invitrogen, Carlsbad, CA). 4,6′-Diamidino-2-phenylindole (DAPI) was used to stain nuclear material. Images were collected using a Zeiss (Oberkochen, Germany) Axiovert 200M wide-field fluorescence microscope equipped with DAPI, fluorescein isothiocyanate, YFP, and tetramethylrhodamine isothiocyanate filter sets and a Plan-Fluar 100×/1.45 numerical aperture (NA) oil objective and a Hamamatsu C4742-95 charge-coupled device (CCD) camera. Images were collected, deconvolved, and adjusted for phase-contrast using Volocity software (PerkinElmer, Waltham, MA). In addition, a Leica TCS SP5 inverted confocal microscope with a 100×/NA 1.4 oil objective was used. Superresolution images were obtained by Applied Precision (Issaquah, WA) DeltaVision-OMX three-dimensional structured illumination using a 100× objective and electron-multiplying CCD camera. All live *Xenopus* images were collected with a Yokogawa CSU-X1M 5000 spinning-disk confocal on a Zeiss Axio Observer inverted motorized microscope with a Zeiss 63×/1.4 NA Plan Apo 1.4 oil objective. Images were acquired with a Hamamatsu OCRA R2 CCD camera controlled with Zen software (Zeiss). For time lapse, images were collected every 1–2 s for 3 min, using an exposure time of 800–900 ms.

Trichostatin A treatment

Parasites grown for 18 h in confluent HFF cells were treated with 100 nM trichostatin A (TSA; Sigma-Aldrich) in growth medium for 1 h. The parasites were 100% methanol fixed before IFA.

Transmission electron microscopy

Parasites transiently transfected with tub-EB1^{Q117A}-YFP/sagCAT were grown overnight in a T25 tissue culture flask confluent with HFF cells. The intracellular parasites were collected by trypsinizing the monolayer and fixed with 2.5% glutaraldehyde in 0.1 M phosphate buffer, pH 7.2. The samples were fixed in OsO_4, dehydrated in ethanol, treated with propylene oxide, and embedded in Spurr's epoxy resin. Sections were stained with uranyl acetate and lead citrate before examination in a JEOL 1200 EX electron microscope (Ferguson *et al.*, 1999).

Western blot

Parasites were grown in the presence and absence of ATc and harvested at various time points. After three washes with phosphate-buffered saline, parasites were lysed by resuspension in buffer containing 50 mM Tris-HCl, pH 7.8, 150 mM NaCl, 1% SDS, and 1× protease inhibitor cocktail (Sigma-Aldrich, St. Louis, MO) and heating at 95°C for 10 min. Parasites at 15 million/lane were loaded and analyzed by SDS–PAGE. The nitrocellulose blot was probed with mouse anti–cMyc-horseradish peroxidase (1:2000; Santa Cruz Biotechnology, Dallas, TX) and mouse anti-α-tubulin 12G10 (Developmental Studies Hybridoma Bank, University of Iowa, Iowa City, IA).

Expression of TgEB1 in *X. laevis*

mRNAs generated from TgEB1 constructs were injected into dorsal blastomeres of *X. laevis* embryos at the two- and four-cell stage (in 0.1× Marc's modified Ringer's: 0.1 M NaCl, 2 mM KCl, 1 mM $MgSO_4$, 2 mM $CaCl_2$, 5 mM 4-(2-hydroxyethyl)-1-piperazineethanesulfonic acid, pH 7.8, 0.1 mM EDTA) with 5% Ficoll) with total mRNA ranging from 25 to 100 pg/embryo. The embryos were dissected at stages 22–24 (Tanaka and Kirschner, 1991; Lowery *et al.*, 2013), and neural tubes were plated in culture medium on laminin-coated (20 μg/ml) coverslips attached to a plastic dish with a whole in the center. For whole-mount imaging, embryos were secured between two thin coverslips, with emphasis on the epithelial cells being the center of focus.

ACKNOWLEDGMENTS

We thank Eliza Vasile from the Koch Institute (Cambridge, MA) for assistance with superresolution microscopy and Tiffany Enzenbacher for handling the TgEB1 *Xenopus* expression constructs. This work was supported by National Institutes of Health Grants MH095768 to L.A.L., AI067981 to N.S.M., and AI107475, AI081924, and AI110690 to M.J.G.

REFERENCES

Akhmanova A, Steinmetz MO (2008). Tracking the ends: a dynamic protein network controls the fate of microtubule tips. Nat Rev Mol Cell Biol 9, 309–322.

Anderson-White BR, Beck JR, Chen CT, Meissner M, Bradley PJ, Gubbels MJ (2012). Cytoskeleton assembly in Toxoplasma gondii cell division. Int Rev Cell Mol Biol 298, 1–31.

Anderson-White BR, Ivey FD, Cheng K, Szatanek T, Lorestani A, Beckers CJ, Ferguson DJ, Sahoo N, Gubbels MJ (2011). A family of intermediate filament-like proteins is sequentially assembled into the cytoskeleton of Toxoplasma gondii. Cell Microbiol 13, 18–31.

Beinhauer JD, Hagan IM, Hegemann JH, Fleig U (1997). Mal3, the fission yeast homologue of the human APC-interacting protein EB-1 is required for microtubule integrity and the maintenance of cell form. J Cell Biol 139, 717–728.

Bieling P, Laan L, Schek H, Munteanu EL, Sandblad L, Dogterom M, Brunner D, Surrey T (2007). Reconstitution of a microtubule plus-end tracking system in vitro. Nature 450, 1100–1105.

Brooks CF, Francia ME, Gissot M, Croken MM, Kim K, Striepen B (2011). Toxoplasma gondii sequesters centromeres to a specific nuclear region throughout the cell cycle. Proc Natl Acad Sci USA 108, 3767–3772.

Bu W, Su LK (2001). Regulation of microtubule assembly by human EB1 family proteins. Oncogene 20, 3185–3192.

Chen CT, Gubbels MJ (2013). The Toxoplasma gondii centrosome is the platform for internal daughter budding as revealed by a Nek1 kinase mutant. J Cell Sci 126, 3344–3355.

Dubremetz JF (1973). Ultrastructural study of schizogonic mitosis in the coccidian, Eimeria necatrix (Johnson 1930) [in French]. J Ultrastruct Res 42, 354–376.

Farrell M, Gubbels MJ (2014). The Toxoplasma gondii kinetochore is required for centrosome association with the centrocone (spindle pole). Cell Microbiol 16, 78–94.

Ferguson D, Cesbron-Delauw MF, Dubremetz JF, Sibley LD, Joiner KA, Wright S (1999). The expression and distribution of dense granule proteins in the enteric (Coccidian) forms of Toxoplasma gondii in the small intestine of the cat. Exp Parasitol 91, 203–211.

Ferguson DJP, Dubremetz JF (2013). The ultrastructure of Toxoplasma gondii. In: Toxoplasma gondii: The Model Apicomplexan, ed. LM Weiss and K Kim, San Diego, CA: Elsevier Academic Press, 19–59.
Francia ME, Jordan CN, Patel JD, Sheiner L, Demerly JL, Fellows JD, de Leon JC, Morrissette NS, Dubremetz JF, Striepen B (2012). Cell division in Apicomplexan parasites is organized by a homolog of the striated rootlet fiber of algal flagella. PLoS Biol 10, e1001444.
Francia ME, Striepen B (2014). Cell division in apicomplexan parasites. Nat Rev Microbiol 12, 125–136.
Gubbels MJ, Morrissette NS (2013). The cytoskeleton: structures and motility. In: Toxoplasma gondii: The Model Apicomplexan, ed. LM Weiss and K Kim, San Diego, CA: Elsevier Academic Press, 455–503.
Gubbels MJ, Vaishnava S, Boot N, Dubremetz JF, Striepen B (2006). A MORN-repeat protein is a dynamic component of the Toxoplasma gondii cell division apparatus. J Cell Sci 119, 2236–2245.
Hartmann J, Hu K, He CY, Pelletier L, Roos DS, Warren G (2006). Golgi and centrosome cycles in Toxoplasma gondii. Mol Biochem Parasitol 145, 125–127.
Hubbert C, Guardiola A, Shao R, Kawaguchi Y, Ito A, Nixon A, Yoshida M, Wang XF, Yao TP (2002). HDAC6 is a microtubule-associated deacetylase. Nature 417, 455–458.
Huynh MH, Carruthers VB (2009). Tagging of endogenous genes in a Toxoplasma gondii strain lacking Ku80. Eukaryot Cell 8, 530–539.
Iimori M, Ozaki K, Chikashige Y, Habu T, Hiraoka Y, Maki T, Hayashi I, Obuse C, Matsumoto T (2012). A mutation of the fission yeast EB1 overcomes negative regulation by phosphorylation and stabilizes microtubules. Exp Cell Res 318, 262–275.
Jacot D, Daher W, Soldati-Favre D (2013). Toxoplasma gondii myosin F, an essential motor for centrosomes positioning and apicoplast inheritance. EMBO J 32, 1702–1716.
Janke C, Bulinski JC (2011). Post-translational regulation of the microtubule cytoskeleton: mechanisms and functions. Nat Rev Mol Cell Biol 12, 773–786.
Janke C, Kneussel M (2010). Tubulin post-translational modifications: encoding functions on the neuronal microtubule cytoskeleton. Trends Neurosci 33, 362–372.
Kline-Smith SL, Sandall S, Desai A (2005). Kinetochore-spindle microtubule interactions during mitosis. Curr Opin Cell Biol 17, 35–46.
Komaki S, Abe T, Coutuer S, Inze D, Russinova E, Hashimoto T (2010). Nuclear-localized subtype of end-binding 1 protein regulates spindle organization in Arabidopsis. J Cell Sci 123, 451–459.
Komarova Y, De Groot CO, Grigoriev I, Gouveia SM, Munteanu EL, Schober JM, Honnappa S, Buey RM, Hoogenraad CC, Dogterom M, *et al.* (2009). Mammalian end binding proteins control persistent microtubule growth. J Cell Sci 184, 691–706.
Kosugi S, Hasebe M, Tomita M, Yanagawa H (2009). Systematic identification of cell cycle-dependent yeast nucleocytoplasmic shuttling proteins by prediction of composite motifs. Proc Natl Acad Sci USA 106, 10171–10176.
Lai R, Bekessy A, Chen CC, Walsh T, Barnard R (2003). Megaprimer mutagenesis using very long primers. Biotechniques 34, 52–5456.
Lee L, Tirnauer JS, Li J, Schuyler SC, Liu JY, Pellman D (2000). Positioning of the mitotic spindle by a cortical-microtubule capture mechanism. Science 287, 2260–2262.
Li R, Gundersen GG (2008). Beyond polymer polarity: how the cytoskeleton builds a polarized cell. Nat Rev Mol Cell Biol 9, 860–873.
Ligon LA, Shelly SS, Tokito M, Holzbaur EL (2003). The microtubule plus-end proteins EB1 and dynactin have differential effects on microtubule polymerization. Mol Biol Cell 14, 1405–1417.
Lin JR, Mondal AM, Liu R, Hu J (2012). Minimalist ensemble algorithms for genome-wide protein localization prediction. BMC Bioinformatics 13, 157.
Lowery LA, Stout A, Faris AE, Ding L, Baird MA, Davidson MW, Danuser G, Van Vactor D (2013). Growth cone-specific functions of XMAP215 in restricting microtubule dynamics and promoting axonal outgrowth. Neural Dev 8, 22.
Maurer SP, Fourniol FJ, Bohner G, Moores CA, Surrey T (2012). EBs recognize a nucleotide-dependent structural cap at growing microtubule ends. Cell 149, 371–382.
Megraw TL, Kaufman TC (2000). The centrosome in Drosophila oocyte development. Curr Top Dev Biol 49, 385–407.
Montoya JG, Liesenfeld O (2004). Toxoplasmosis. Lancet 363, 1965–1976.
Morlon-Guyot J, Berry L, Chen CT, Gubbels MJ, Lebrun M, Daher W (2014). The Toxoplasma gondii calcium-dependent protein kinase 7 is involved in early steps of parasite division and is crucial for parasite survival. Cell Microbiol 16, 95–114.
Morrissette NS, Sibley LD (2002). Disruption of microtubules uncouples budding and nuclear division in Toxoplasma gondii. J Cell Sci 115, 1017–1025.
Nishi M, Hu K, Murray JM, Roos DS (2008). Organellar dynamics during the cell cycle of Toxoplasma gondii. J Cell Sci 121, 1559–1568.
Piperno G, LeDizet M, Chang XJ (1987). Microtubules containing acetylated alpha-tubulin in mammalian cells in culture. J Cell Biol 104, 289–302.
Roos DS, Donald RG, Morrissette NS, Moulton AL (1994). Molecular tools for genetic dissection of the protozoan parasite Toxoplasma gondii. Methods Cell Biol 45, 27–63.
Schwartz K, Richards K, Botstein D (1997). BIM1 encodes a microtubule-binding protein in yeast. Mol Biol Cell 8, 2677–2691.
Sheiner L, Demerly JL, Poulsen N, Beatty WL, Lucas O, Behnke MS, White MW, Striepen B (2011). A systematic screen to discover and analyze apicoplast proteins identifies a conserved and essential protein import factor. PLoS Pathog 7, e1002392.
Shen B, Brown KM, Lee TD, Sibley LD (2014). Efficient gene disruption in diverse strains of Toxoplasma gondii using CRISPR/CAS9. MBio 5, e01114.
Sidik SM, Hackett CG, Tran F, Westwood NJ, Lourido S (2014). Efficient genome engineering of Toxoplasma gondii using CRISPR/Cas9. PLoS One 9, e100450.
Striepen B, Crawford MJ, Shaw MK, Tilney LG, Seeber F, Roos DS (2000). The plastid of Toxoplasma gondii is divided by association with the centrosomes. J Cell Biol 151, 1423–1434.
Strobl JS, Cassell M, Mitchell SM, Reilly CM, Lindsay DS (2007). Scriptaid and suberoylanilide hydroxamic acid are histone deacetylase inhibitors with potent anti-Toxoplasma gondii activity in vitro. J Parasitol 93, 694–700.
Tanaka EM, Kirschner MW (1991). Microtubule behavior in the growth cones of living neurons during axon elongation. J Cell Biol 115, 345–363.
Tran JQ, Li C, Chyan A, Chung L, Morrissette NS (2012). SPM1 stabilizes subpellicular microtubules in Toxoplasma gondii. Eukaryot Cell 11, 206–216.
Vaishnava S, Morrison DP, Gaji RY, Murray JM, Entzeroth R, Howe DK, Striepen B (2005). Plastid segregation and cell division in the apicomplexan parasite Sarcocystis neurona. J Cell Sci 118, 3397–3407.
Verhey KJ, Gaertig J (2007). The tubulin code. Cell cycle 6, 2152–2160.
Xiao H, El Bissati K, Verdier-Pinard P, Burd B, Zhang H, Kim K, Fiser A, Angeletti RH, Weiss LM (2010). Post-translational modifications to Toxoplasma gondii alpha- and beta-tubulins include novel C-terminal methylation. J Proteome Res 9, 359–372.